

# NATIONAL ADVISORY COMMITTEE FOR AERONAUTICS

TECHNICAL NOTE 3989

STRENGTH AND DUCTILITY OF BAINITIC STEELS

By Donald H. Desy, J. O. Brittain, and M. Gensamer

Columbia University



Washington  
August 1957

---

TECHNICAL NOTE 3989

---

STRENGTH AND DUCTILITY OF BAINITIC STEELS

By Donald H. Desy, J. O. Brittain, and M. Gensamer

SUMMARY

Some of the factors believed to affect the strength and ductile-to-brittle transition temperature of bainitic steels, including mean ferrite path and degree of internal strain, have been studied. Strength was measured by diamond pyramid hardness, and transition temperature was obtained from a tensile impact test on small notched specimens. Seven laboratory heats of carbon-molybdenum steel and two heats of carbon steel were transformed isothermally to bainite at various temperatures and tested. Mean-ferrite-path measurements were made on electron micrographs of three of these steels. The mean ferrite path was found to have only a slight effect on the strength of bainite and no effect on the transition temperature. Preliminary measurements of X-ray line broadening indicate that the degree of internal strain may be the controlling factor in determining the strength of bainite. The transition temperatures of the bainites fell within a band between  $-80^{\circ}$  and  $-160^{\circ}$  C and did not vary regularly with hardness, carbon or alloy content, or mean ferrite path. In the SAE 1062 steel at high strength levels, bainite has a transition temperature lower than that of tempered martensite at the same strength level.

INTRODUCTION

In recent years, it has become increasingly necessary in the aircraft industry to employ steel in heavy sections. Since it is highly desirable that steels used in such sections have optimum strength and ductility, it is necessary to investigate means for improving these properties. The mass of such sections generally precludes the possibility of quenching to produce a martensitic microstructure. Instead, these sections usually have pearlitic or bainitic microstructures. A bainitic structure, because of its high strength which is comparable to that of tempered martensite, is frequently desirable in heavy steel sections.

Some of the factors believed to influence the strength and ductility of bainites were studied in this investigation. These factors are transformation temperature, carbon and alloy content, quantitative microstructure, and degree of internal strain. In general, what is meant by

quantitative microstructure is some measure of the degree of dispersion or spacing of hard particles in a softer matrix in a two-phase alloy. For steels, the measure of quantitative microstructure generally used is the mean ferrite path, which will be described in a later section.

Previous work has indicated the importance of quantitative microstructure in influencing the strength of steels having a structure of pearlite, spheroidite, and mixtures of ferrite and pearlite (refs. 1 to 3), of aluminum alloys (ref. 4), and of various other alloys and aggregates (ref. 5). For this reason, a large portion of the present investigation was devoted to the determination of the mean ferrite path in bainite and its relationship to the strength of the material. The effect of quantitative microstructure on the ductile-to-brittle transition temperature in steels having a microstructure of pearlite, spheroidite, and mixtures of ferrite and pearlite has given contradictory results as studied by various investigators (refs. 6 to 12). In this investigation, an effort was made to determine whether a general relationship between mean ferrite path and transition temperature exists in bainitic steels.

The experimental work was conducted on a series of small laboratory heats of steel which vary in carbon and molybdenum content and on a heat of commercial SAE 1062 steel. Specimens of these steels were transformed isothermally to bainite. Mechanical testing consisted of hardness tests and of tensile impact tests over a temperature range sufficiently broad to establish the transition temperature. Some slow tensile tests were also made. For three of the steels, mean-ferrite-path measurements were made on electron micrographs of bainite formed over a range of temperatures. This investigation was conducted at Columbia University under the sponsorship and with the financial assistance of the National Advisory Committee for Aeronautics. The authors wish to thank Dr. F. Garofalo, Mr. L. Zwell, and Mr. R. J. Kosinski of the United States Steel Research Laboratory, Kearney, N. J., as well as Dr. D. H. Gurinsky, Mr. O. F. Kammerer, and Mr. J. Sadofsky of Brookhaven National Laboratory, for preparation of the X-ray spectrometer traces used in this report, and they wish especially to acknowledge the valuable contributions of Miss B. L. Hammond, who tested specimens and prepared the electron micrographs. Steel A was supplied by the Page Steel and Wire Division of the American Chain and Cable Co. Thanks are also due to Mr. L. C. Weiner and the many other members of the Metallurgical Laboratories of the School of Mines in Columbia University who willingly contributed their services.

## APPARATUS AND PROCEDURE

## Materials and Heat Treatment

The steels tested in this investigation contained relatively small amounts of alloying elements, not much more than enough to provide enough hardenability to permit the necessary heat treatments. They included a series of carbon-molybdenum heats containing from 0.20 to 0.40 percent carbon and from 0.25 to 1.00 percent molybdenum. Molybdenum was chosen because of its effect in increasing the time for the beginning of the pearlite transformation, thus facilitating quenching the specimens into the bainite transformation-temperature range. Manganese, silicon, and aluminum were maintained constant in these steels. Heats of about 200 grams were melted in an argon atmosphere using a high-frequency induction furnace which was adaptable for either vacuum or inert-gas melting. The steels were then homogenized and cold-swaged to 3/16-inch diameter, with intermediate anneals in vacuum. A 0.47-percent-carbon, 0.67-percent-manganese steel, melted under argon, was hot swaged after plating with copper and nickel for protection from the atmosphere. In addition, a commercial silicon-killed SAE 1062 steel received in the form of straightened and cut 3/16-inch-diameter wire was included in the testing program. The chemical composition of the steels used in this investigation is given in table I.

The time necessary for completion of isothermal transformation at a given temperature was determined by microscopic examination of preliminary specimens which had been heat-treated isothermally in lead baths. It was found necessary to homogenize the steels of higher carbon and alloy content a second time to eliminate segregation, which had prevented the specimens from transforming completely to bainite. Some specimens of steel 17 were homogenized at 1,050° C for 6 hours; steels 19, 20, 21, and 22 were homogenized at 1,050° C for 15 hours or more. After segregation had been eliminated by this means, the specimens were austenitized for 1/2 hour in a lead bath (at 900° C for the molybdenum steels and at 843° C for steels A and B-19), then quenched rapidly into another lead bath at the desired temperature and held until completion of transformation to bainite or pearlite.

## Hardness and Strength Tests

Diamond-pyramid-hardness tests were made on a standard Tukon hardness tester, using a 3-kilogram load. At least five hardness impressions were made on each specimen. Tensile tests were made on some specimens of steel A which had been isothermally transformed to bainite and on others which had been quenched to martensite and tempered. Logarithm of true stress was plotted against logarithm of true strain for these

specimens. Stress at 0.015 strain was chosen as a reliable strength parameter at the strength levels developed in this steel. Engineering tensile strength was also computed from the test results.

### Tensile Impact Testing

Tensile impact tests to determine the ductile-to-brittle transition temperature were performed at temperatures down to that of liquid nitrogen. The specimen was  $3/16$  inch in diameter, with 48 threads per inch over its entire length, and five to seven circumferential notches spaced at intervals of  $3/8$  inch. The specimens were prenotched before heat treatment, then finished after heat treatment with a carbide-tipped tool bit honed to the sharpest possible edge with diamond paste. In this way, it was possible to produce notches having a radius ranging from less than 0.0005 inch to about 0.0015 inch. In this range, variation in the notch sharpness does not seem to affect the ductility. The notch angle was  $60^\circ$ .

The specimens were broken in the machine shown in figure 1. The lower portion of the machine, in which the specimens were gripped and cooled, is shown in detail in figure 2. The weight, after sliding down the rod, struck the sleeve with 40 foot-pounds of energy, which was usually sufficient to break the specimen in one blow. Occasionally, it was necessary to drop the weight a second time. The specimens were cooled by a stream of gaseous nitrogen, which had been cooled by being passed through a copper coil immersed in a Dewar flask containing liquid nitrogen. Temperature control was achieved by regulating the rate of gas flow. A copper-constantan thermocouple was inserted through a hole in the lower grip with its junction about 2 millimeters from the notch. Calibration against another thermocouple attached to the root of the notch showed a constant difference of 0.03 millivolt ( $1^\circ$  to  $1.5^\circ$  C) between these two spots while the specimen was being cooled by a stream of nitrogen. This correction was therefore applied to all such tests. For somewhat higher temperatures than those attained by this method, a bath of dry ice and trichloroethylene was used. For still higher temperatures, water or oil baths were used. No correction for position of thermocouple was needed when baths were employed. All specimens were held at constant temperature for 1 to 2 minutes before breaking. The thermocouple was calibrated at liquid-nitrogen temperature ( $-195.8^\circ$  C), dry-ice and trichloroethylene temperature ( $-78^\circ$  C), and at  $0^\circ$  C. From the calibration curve so obtained, a correction was applied to all temperature measurements. As a result, they are believed to be accurate within  $\pm 1^\circ$  C at the instant the specimen is broken.

Before the specimens were broken, the diameter at the root of the notch was measured to within 0.0001 inch on an optical comparator. At least three diameters were measured for each notch, and these were

averaged. After fracture, the diameter was measured by means of a microscope furnished with a micrometer stage capable of an accuracy of 0.0001 inch, and, again, the average of three diameters was taken. This was found necessary for two reasons: First, the notch was sometimes slightly elliptical because of inaccuracy in machining; second, after fracture it was sometimes deformed into an ellipse. The percent reduction in area was then computed from these measurements and plotted against test temperature. At least 10 points are needed to establish a transition temperature. However, about twice this many are desirable because of the scatter inherent in the nature of the test, especially in the range of the transition temperature. This is true of standard Charpy and Izod tests, as well as of the tensile impact tests employed here. Further uncertainty was introduced in these tests by the difficulty in making measurements of the diameter of the fracture at the root of the notch, especially for some of the specimens in which the fracture occurred partially outside the root of the notch.

Typical transition-temperature curves are shown in figure 3. A transition-temperature plot usually has three branches, an upper branch representing the maximum ductility, a more or less sharply sloping middle branch showing where the transition from ductile to brittle behavior occurs, and a lower branch representing the minimum ductility of the material. In some of the plots in figure 3, only the middle and lower branches are shown. The transition temperature is taken as the temperature at the intersection of the middle and lower branches. For consistency in determining the transition temperature, it was considered desirable to select a constant value of minimum ductility, consistent with the data, for each group of specimens tested. This value was set at zero reduction in area for steels A and B-19, at 1 percent reduction in area for the remaining bainitic steels, and at 3 percent reduction in area for steel 25 in the pearlitic condition. The accuracy to be expected in the determination of the transition temperature depends upon the steel tested and the number of points taken. The higher the carbon and strength level of the steel, the less the difference in ductility between brittle and ductile specimens will be and the less rapid the change in ductility as shown by the middle branch of the curve. With sufficient points (at least 20 for the higher carbon steels) it is believed that the transition temperature can be established to within  $\pm 20^{\circ}$  C.

A comparison between the transition temperature as obtained by the tensile impact test and by the standard V-notch Charpy test from the same material showed good correlation between the results of the two tests. The steels tested were a fully killed as-rolled SAE 1020 steel, a semi-killed as-rolled SAE 1020 steel, and a steel having the composition 0.162 percent carbon, 1.21 percent manganese, and 0.32 percent silicon in as-rolled condition. The criteria for transition temperature which were compared in the two tests were the temperature at 15 foot-pounds for the V-notch Charpy test and the temperature at the intersection of

the lower branch of the curve with the middle branch for the tensile impact test. The difference in the transition temperature found by the two methods varied from 0° to 40° F (0° to 22° C), which is approximately the precision with which transition temperature could be obtained by the tensile impact test alone.

#### Mean-Ferrite-Path Measurements

Electron micrographs were prepared from specimens of steels A, 16, and 22 which were heat-treated to produce bainite and tested in tensile impact. The techniques employed were those recommended in reference 13. Briefly, the method is as follows: Longitudinal sections were mechanically polished using standard metallographic techniques, then lightly etched in saturated picral plus Zephiran chloride and repolished several times to remove the surface layer of disturbed metal. After the final etch, replicas of parlodion or collodion were prepared and shadowed at 30° with palladium to provide contrast. For each specimen electron micrographs of 20 random areas were made. The magnification used was between 2600 and 13,500 diameters depending on the structure studied and was chosen so as to define the carbide particles clearly and to include a sufficient number of particles in the area so that accurate mean-ferrite-path measurements could be made. From the original plates intermediate negatives were made; enlargements at a magnification of two diameters then were made from these. Typical electron micrographs are shown in figure 4.

The mean ferrite path is defined as the arithmetic mean of the distance between carbide particles in a ferrite matrix averaged for all directions through the specimen. This measurement may be made directly on the electron micrographs by measuring the distances between carbide particles along a number of lines drawn in different directions on the print and averaging these distances. This procedure is tedious, however, and, since the percentage composition is known, the measurement can be simplified by means of the principle of lineal analysis.

It is shown by this principle that the volume fraction of a given constituent in an aggregate is equal to that fraction of a mean straight line passing through the aggregate which intercepts that constituent; that is, volume fraction equals lineal fraction. Consider a unit mean line passing through a ferrite-carbide aggregate. Then the sum of the line segments passing through the ferrite will be equal to the volume fraction of ferrite, and the sum of the line segments passing through the carbides will be equal to the volume fraction of the carbide. If there are  $n$  segments of the unit line passing through ferrite, then the mean ferrite path is given by the volume fraction of ferrite divided by  $n$ . Since the volume fraction of ferrite can be computed from composition, it is only necessary to count the number of ferrite intercepts

per unit distance on a sufficiently large number of lines drawn on electron micrographs of the material. For each specimen, ferrite intercepts along 18 lines in 6 directions were counted on each of 20 electron micrographs. The precision of the mean-ferrite-path measurements, represented as 95 percent confidence limits for each specimen, was between 5 and 10 percent. (Standard statistical methods were used in calculating confidence limits.)

### X-Ray Diffraction

X-ray diffraction studies were made on specimens of steel 22 isothermally transformed to bainite at 350° and 480° C and to pearlite at 680° C. Spectrometer traces were made of the (110) and the (211) reflections using iron-filtered cobalt  $K_{\alpha}$  radiation and a scanning rate of 0.2° per minute. Since the above traces showed differences in line breadth, the following specimens of steel A were prepared for further X-ray diffraction studies of this phenomenon. Specimens were isothermally transformed to bainite at 300°, 350°, 400°, and 450° C and air-cooled after transformation. Additional specimens were water-quenched after transformation at 300° and 450° C. One specimen was normalized by air-cooling from 860° C and stress relieved at 550° C followed by air-cooling. Normalized specimens were also cold-drawn into wire from an original diameter of 3/16 inch to a final diameter of 0.032 inch for a total reduction of area of 97.2 percent. X-ray spectrometer traces of the (211) reflection were made on the heat-treated specimens and on specimens cold-drawn 37.6, 76.0, 94.1, and 97.2 percent. Iron-filtered cobalt  $K_{\alpha}$  radiation and a scanning rate of 1/8° per minute were used. Diamond-pyramid-hardness measurements were made on all the above specimens.

## RESULTS AND DISCUSSION

### Strength and Hardness of Bainites

For bainite formed isothermally from steel A, diamond pyramid hardness was plotted against tensile strength (fig. 5). From this plot a linear relationship was determined. True stress at a true strain of 0.015 when plotted against hardness also gives a straight-line relationship (fig. 6). Similar relationships were found for tempered martensite formed from the same steel. These data merely confirm the well-known correlation between hardness and strength (refs. 14 and 15). Since the two properties are so closely related, they will be spoken of interchangeably hereafter.

In figure 7 diamond pyramid hardness has been plotted against isothermal transformation temperature for the nine bainitic steels tested in

this investigation. Steels of varying carbon contents tend to fall on separate straight lines, with the higher carbon steels in general having a higher hardness at a given transformation temperature. At low transformation temperatures in the vicinity of 350° C, however, the difference in the hardness between high- and low-carbon steels becomes insignificant.

Figure 8 shows the relationship of hardness to logarithm of mean ferrite path for bainites as compared with the same relationship for pearlite, spheroidite, and mixed ferrite and pearlite (ref. 3). The bainites do not follow a unique relationship of hardness to mean ferrite path, but fall on separate lines depending on carbon content. It will be noted that the slopes of these lines are all greater than the slope for pearlites, spheroidites, and mixed ferrites and pearlites. The significance of these deviations is discussed below.

The logarithm of the mean ferrite path developed in three steels of varying carbon contents transformed to bainite is plotted as a function of transformation temperature in figure 9. The lower the carbon content of the steel, the longer the mean ferrite paths developed at a given transformation temperature. Also, the higher the carbon content of the steel, the less the increase in mean ferrite path with increasing transformation temperature. The change in mean ferrite path with temperature in the 0.60-percent-carbon steel transformed to bainite is quite small, especially when compared with the corresponding change in pearlites, spheroidites, and mixed ferrites and pearlites as shown by Gensamer et al. for steels of similar composition (ref. 2).

Although the mean path between carbide particles in the ferrite matrix may partially account for the hardness of bainite, it is not the major explanation for the hardening. For any particular bainitic steel, the hardness increases linearly and the logarithm of mean ferrite path decreases linearly as the transformation temperature decreases (figs. 7 and 9). Also, the hardness increases as the logarithm of mean ferrite path decreases (fig. 8). However, here the rate of increase of hardness with decreasing mean ferrite path is much greater than that found previously for pearlite, spheroidite, and mixed ferrite and pearlite (refs. 2 and 3). If the hardening rate for pearlite, spheroidite, and mixed ferrite and pearlite with decreasing mean ferrite path is taken as representative of dispersions of iron carbide in iron, then the rapid increase in hardness of bainite for a relatively small decrease in mean ferrite path can not be caused entirely by that decrease in mean ferrite path. On this basis, it appears that the observed correlation of hardness of bainite with mean ferrite path mainly derives from the fact that both of these properties vary with the transformation temperature.

This can also be seen in the following manner. If the mean ferrite path were the most important factor in determining the strength of bainite, then the strength of any bainite, regardless of carbon content, should

be the same at a given value of mean ferrite path. However, figure 8 shows that bainites of differing carbon content have widely different hardness at any given value of mean ferrite path. That is, at a given value of mean ferrite path, the low-carbon bainites are harder than the high-carbon bainites. In addition, a bainite having any given value of mean ferrite path is developed at a lower transformation temperature in the low-carbon steels than in the high-carbon steels, as shown in figure 9. Therefore, it appears that the controlling factor in the strength of bainite is the temperature at which the bainite is formed, rather than the mean ferrite path, in that bainites formed at low transformation temperatures are harder than those formed at higher temperatures.

Since the hardness of bainite is not adequately explained by variations in its mean ferrite path, but is correlated with the temperature at which it is formed, some preliminary studies have been made to determine what other factors which could affect the hardness vary with the transformation temperature. These studies are discussed below.

The matrix of bainite could be strengthened if it contained a non-equilibrium amount of carbon in supersaturated solid solution. This would have the effect of distorting the crystal lattice either by expanding the cubic lattice parameter  $a_0$  or, as in the case of martensite, by formation of a tetragonal lattice. This possibility was investigated by means of X-ray diffraction and by point counting of carbides on electron micrographs.

Back-reflection X-ray spectrometer traces were made on specimens of steel 22 which were heat-treated to produce bainite and pearlite. No difference in lattice parameter was found among these specimens, or between them and a standard National Research Corp. iron specimen. Also, examination of the X-ray diffraction pattern revealed no evidence of the formation of a tetragonal structure.

In order to account for the hardness difference between the hardest and softest bainite developed in steel 22, about 0.25 percent carbon in solution would be required, an amount which produces similar hardening in martensite. Since steel 22 contained 0.35 percent total carbon by chemical analysis, this would leave only 0.10 percent carbon as carbides. Point-counting measurements gave a result of 0.55 percent carbon as carbides for lower bainite and 0.86 percent for upper bainite. This carbon discrepancy in the direction of high carbon is to be expected, since the etching of the specimen and shadowing of the replica cause the carbides to occupy an area greater than they would on a perfectly plane section, which is assumed in the point-counting technique; larger particles are more deeply etched and cast larger shadows, so that the apparent area of the carbides would be increased in this way. It would therefore be expected that for a steel of the same carbon content, the specimen containing larger carbides (upper bainite) would give a higher positive

error in carbon content by point counting than would the specimen with small particles (lower bainite). These results confirm the X-ray data and show that the hardness of bainite is not caused by excess carbon in solution in the matrix.

Another mechanism for the hardening of bainite was suggested by the line broadening shown in the X-ray spectrometer traces of the bainites and pearlite formed in steel 22 (as discussed in a private communication from Messrs. F. Garafalo, L. Zwell, and R. J. Kosinski). The difference in line breadth between specimens was attributed to varying degrees of internal stress. The lower bainite showed the greatest amount of line broadening, then upper bainite and pearlite, in that order. Since this parallels the hardness of the three specimens, the degree of internal stress may be an important factor in the hardening of bainite.

Line-breadth measurements at half maximum intensity were made on spectrometer traces of the (211) ferrite reflection from steel A transformed to bainite at various temperatures as well as on one normalized specimen. These values were plotted against diamond pyramid hardness in figure 10. The same variables were also plotted in this figure for steel A hardened by cold-work. A straight-line relationship exists between hardness and line breadth in the bainitic steels. The point for the normalized specimen also falls on this line. The points for the cold-worked specimens fall on a separate straight line, which crosses the line for the heat-treated specimens and has a steeper slope. Line breadth is a measure of some form of internal strain. (The contribution of particle size to the line broadening in these specimens is believed to be small.)

The internal strains in bainite undoubtedly have their origin in the subcritical transformation of austenite to bainite. The bainites formed at lower temperatures would be expected to retain a greater proportion of the strains introduced by the austenite-to-bainite transformation because the degree of stress relief is less at lower temperatures. No appreciable strain is introduced by water-quenching the specimens after the bainite transformation is completed, as is shown by the duplicate points on the graph at 330 and 580 diamond-pyramid-hardness number (DPN) which represent specimens air-cooled and water-quenched from 450° and 300° C, respectively. The strains introduced by cold-work are very probably distributed in a different manner from those caused by the transformation of austenite to bainite at subcritical temperatures, so that a different dependence of hardness on line breadth is to be expected. However, the similarity in the relation of hardness to line breadth between cold-worked and bainitic specimens of the same steel gives support to the hypothesis that bainite is strengthened primarily by internal strain.

## Ductility (Transition Temperature) of Bainite

The results of impact and hardness tests on all steels as well as the mean-ferrite-path measurements for steels A, 16, and 22 are shown in table II. In addition to the transition-temperature value as defined previously, the percent reduction in area at  $-50^{\circ}\text{C}$  and the temperature at 4-percent reduction in area are recorded. This temperature,  $-50^{\circ}\text{C}$ , was chosen as approximating the minimum which aircraft steels are likely to encounter in service. The temperature at which the ductility of the steels first rose to 4-percent reduction in area was chosen as an alternate transition temperature, one at which the material still retains some ductility.

The transition temperature of 0.20-percent-carbon bainites has been plotted against isothermal transformation temperature in figure 11(a). Pearlites, developed in a steel of 0.20 percent carbon and 0.50 percent molybdenum between  $575^{\circ}$  and  $675^{\circ}\text{C}$ , have been included for comparison. The molybdenum content in the three steels tested was 0.24, 0.50, and 1.02 percent, respectively. The graph shows nearly identical behavior for the three steels regardless of molybdenum content. For these steels, there is a linear increase in transition temperature with increasing transformation temperature. This regular relationship is not followed by steels of higher carbon content, as shown in figures 11(b) to 11(d). The exceptionally high point at  $30^{\circ}\text{C}$  for steel 22 is not believed to be a true effect but to be due to lack of sufficient specimens to establish the transition temperature correctly. Figure 11(d) for steel A includes three points for pearlites (at  $550^{\circ}$ ,  $600^{\circ}$ , and  $650^{\circ}\text{C}$ ) which have higher transition temperatures than bainites in the same steel. Except for the 0.20-percent-carbon steels, the data do not show any regular variation of transition temperature with transformation temperature. However, for all bainites tested, the transition temperature fell between  $-80^{\circ}$  and  $-160^{\circ}\text{C}$ , except for the above-mentioned high point and one point at  $-175^{\circ}\text{C}$ . From a practical point of view, this is considered to be an important result.

When transition temperature is plotted against hardness for all steels tested (fig. 12) it is seen that, in general, the points fall within a band between  $-80^{\circ}$  and  $-160^{\circ}\text{C}$ . There does not seem to be any trend in transition temperature over the entire hardness range. For hardness increasing from 250 to 350 diamond pyramid number, there appears to be a trend toward decreasing transition temperatures. This is because the 0.20-percent-carbon steels, which fall in this hardness range, show a decrease in transition temperature with decreasing transformation temperature.

In figure 13, transition temperature is plotted against logarithm of mean ferrite path for steels A, 22, and 16, which contain 0.60, 0.40, and 0.20 percent carbon, respectively. Within the range of mean-ferrite-path values covered by these three steels, the transition temperature

seems to remain approximately constant except for the 0.20-percent-carbon steel, which shows a rise in transition temperature with increasing mean ferrite path. This behavior in the 0.20-percent-carbon steel parallels the rising trend in transition temperatures as the transformation temperature is increased, as shown in figure 11(a).

It may be concluded that no overall effect on the transition temperature in bainites was exerted by either structure, hardness, or composition of the steel. However, the transition temperatures found in bainite are relatively low and, in addition, are lower than those found in pearlites formed from the same steels.

#### Comparison of the Ductility of Martensite and Bainite

The transition temperature of tempered martensite in steel A is plotted against tempering temperature in figure 14. The transition temperature falls sharply as the tempering temperature increases from 350° to about 425° C, and then levels off or rises slightly at higher tempering temperatures. This is typical of the behavior of martensite in most steels. The lack of ductility for the lower tempering temperatures is a result of the phenomenon of "500° F embrittlement," which though found in most quenched and tempered steels does not occur in bainite. A comparison of the ductility of bainite and martensite in figure 15 shows the marked superiority of bainite at higher strength levels.

#### CONCLUSIONS

The following conclusions were derived from the present investigation of the strength and ductility of bainitic steels:

1. The strength of a bainitic steel at a given carbon level is linear with respect to its isothermal transformation temperature. At the higher transformation temperatures, the hardness increases with the carbon content; but, at lower transformation temperatures, the difference in hardness between high- and low-carbon bainite is insignificant.

2. Mean ferrite path is not an important factor in the strength of bainites, as it is for pearlites, spheroidites, and pearlite-ferrite mixtures. Internal strain may be the controlling factor in the strength of bainite.

3. The rate of increase of mean ferrite path with increasing transformation temperature in bainite is greater for low-carbon steels than for high-carbon steels. For a given transformation temperature, the greater mean ferrite path is developed by the low-carbon steel.

4. The ductile-to-brittle transition temperature for bainite in the steels studied falls between  $-80^{\circ}$  and  $-160^{\circ}$  C and does not vary in any regular manner with hardness, carbon or alloy content, or mean ferrite path.

5. In an SAE 1062 steel at high strength levels, bainite has greater ductility (lower transition temperature) than has tempered martensite of the same hardness and strength.

Columbia University,  
New York, N.Y., March 16, 1956.

## REFERENCES

1. Gensamer, M., Pearsall, E. B., and Smith, G. V.: The Mechanical Properties of the Isothermal Decomposition Products of Austenite. Trans. ASM., vol. 28, 1940, pp. 380-398.
2. Gensamer, M., Pearsall, E. B., Pellini, W. S., and Low, J. R., Jr.: The Tensile Properties of Pearlite, Bainite, and Spheroidite. Trans. ASM., vol. 30, 1942, pp. 983-1020.
3. Gensamer, M.: Strength and Ductility. Trans. ASM., vol. 36, 1946, pp. 30-60.
4. Shaw, R. B., Shepard, L. A., Starr, C. D., and Dorn, J. E.: The Effect of Dispersions on the Tensile Properties of Aluminum-Copper Alloys. Trans. ASM., vol. 45, 1953, pp. 249-274.
5. Unckel, H.: The Dependence of Mechanical Properties on Structure in Two Phase Alloys. Metallurgia, vol. 5, 1951, pp. 146-152.
6. Gross, J. H., and Stout, R. D.: The Effect of Microstructure on Notch Toughness - Part I. The Welding Jour., vol. 30, no. 10, Oct. 1951, pp. 481s-485s.
7. Grossman, N.: Pearlitic Structure Effect on Brittle Transition Temperature. The Welding Jour., vol. 28, no. 6, June 1949, pp. 265s-269s.
8. Osborn, C. J., Scotchbrook, A. F., Stout, R. D., and Johnston, B. G.: Comparison of Notch Tests and Brittleness Criteria. The Welding Jour., vol. 28, no. 1, May 1949, pp. 227s-235s.
9. Harris, W. J., Rinebolt, J. A., and Raring, R.: Upper and Lower Transitions in Charpy Test. The Welding Jour., vol. 30, no. 9, Sept. 1951, pp. 417s-422s.
10. Rinebolt, J. A., and Harris, W. J.: The Effect of Alloying Elements on the Notch Toughness of Pearlitic Steels. Trans. ASM., vol. 43, 1951, pp. 1175-1214.
11. Rinebolt, J. A.: The Effect of Pearlite Spacing on Transition Temperature of Steel at Four Carbon Levels. Trans. ASM., vol. 46, 1954, pp. 1527-1543.

12. Baeyertz, M., Craig, W. F., Jr., and Bumps, E. S.: The Effect of Ferrite Grain Structure Upon Impact Properties of 0.80 Percent Carbon Spheroidite. Jour. Metals, vol. 188, no. 12, Dec. 1950, pp. 1465-1471.
13. Subcommittee XI on Electron Microstructure of Steel, ASTM Committee E-4 on Metallography: First Progress Report on Electron Microstructure of Steel. Proc. A.S.T.M., vol. 50, 1950, pp. 444-492.
14. Williams, S. R.: Hardness and Hardness Measurements. A.S.M. (Cleveland), 1942, pp. 47-48.
15. Lysaght, V. E.: Indentation Hardness Testing. Reinhold Pub. Corp., 1949, pp. 134-135.

TABLE I

## CHEMICAL COMPOSITION OF STEELS TESTED

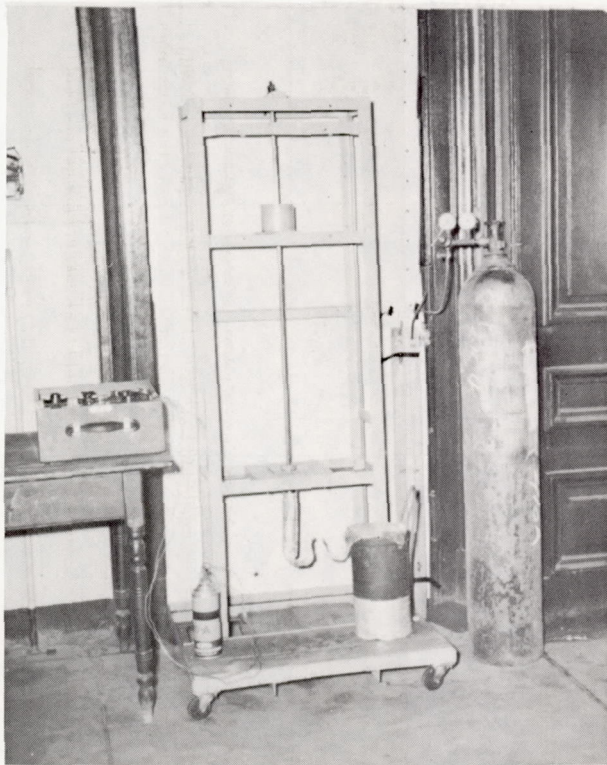
[Iron from National Research Corp., which was basis for all melts except steel A, contained 0.001 percent boron by analysis]

Steel	Element content, percent						
	Carbon, C	Silicon, Si	Manganese, Mn	Molybdenum, Mo	Aluminum, Al	Phosphorus, P	Sulfur, S
15	0.21	0.44	0.76	0.24	0.02	-----	-----
16	.20	.51	.72	.47	.01	-----	-----
17	.20	.44	.74	1.02	.02	-----	-----
19	.30	.44	.75	.51	.02	-----	-----
20	.29	.44	.76	.97	.02	-----	-----
21	.44	.44	.79	.25	.02	-----	-----
22	.35	.42	.74	.50	.01	-----	-----
B-19	.47	.17	.67	----	----	0.007	0.017
A <sup>a</sup>	.60	.145	1.07	----	----	.010	.026

<sup>a</sup>Commercial SAE 1062 steel.

TABLE II  
TEST RESULTS FOR ALL STEELS

Steel	Heat treatment, °C	Transition temperature, °C	Percent reduction in area at -50° C	Temperature at 4-percent reduction in area, °C	Diamond pyramid hardness, DPN	Mean ferrite path, A	Log mean ferrite path	
Isothermal								
A	300	-110	1.0	140	545	1,414	3.150	
	325	-125	1.8	40	509	-----	-----	
	350	-130	2.3	8	469	1,540	3.188	
	375	-140	3.5	-40	427	-----	-----	
	400	-135	3.5	-40	398	1,833	3.263	
	425	-145	3.7	-40	374	-----	-----	
	450	-145	5.2	-70	341	1,906	3.280	
	475	-130	5.5	-70	316	-----	-----	
	500	-140	5.0	-70	313	2,145	3.331	
	550	-75	1.5	-8	---	-----	-----	
	600	-115	5.3	-65	---	-----	-----	
	650	-60	.5	15	---	-----	-----	
	Tempered							
	A	300	>160	0	---	555	-----	-----
350		60	0	---	524	-----	-----	
375		-10	0	180	502	-----	-----	
425		-150	3.0	-10	452	-----	-----	
450		-140	4.0	-50	431	-----	-----	
500		-180	5.2	-80	375	-----	-----	
550		-130	3.2	-30	340	-----	-----	
Isothermal								
B-19	350	-130	3.2	-30	476	-----	-----	
	400	-140	5.1	-70	391	-----	-----	
	450	-140	2.2	30	323	-----	-----	
15	405	-155	15+	-143	340	-----	-----	
	445	-135	15+	-130	294	-----	-----	
	490	-80	20	-77	259	-----	-----	
16	405	-160	20+	-150	361	5,376	3.731	
	445	-125	20+	-120	301	6,815	3.834	
	490	-100	14	-90	256	10,126	4.005	
17	405	-155	26	-150	348	-----	-----	
	445	-125	36	-125	---	-----	-----	
	490	-85	8	-70	266	-----	-----	
19	385	-100	6	-70	385	-----	-----	
	440	-150	11.5	-120	318	-----	-----	
	490	-130	13	-110	254	-----	-----	
20	370	-175	14	-150	451	-----	-----	
	470	-155	10	-120	320	-----	-----	
21	350	-80	5	-70	507	-----	-----	
	420	-105	20	-100	352	-----	-----	
	475	-115	17	-105	277	-----	-----	
22	350	-110	4.2	-75	467	2,018	3.305	
	420	-115	8.5	-90	333	4,352	3.639	
	480	30	1.0	40	276	5,636	3.751	
25	575	45	3	55	257	-----	-----	
	600	10	3	10	230	-----	-----	
	625	-15	3	-3	183	-----	-----	
	650	25	3	30	187	-----	-----	
	675	55	3	54	195	-----	-----	



L-57-3038

Figure 1.- Tensile impact testing machine.

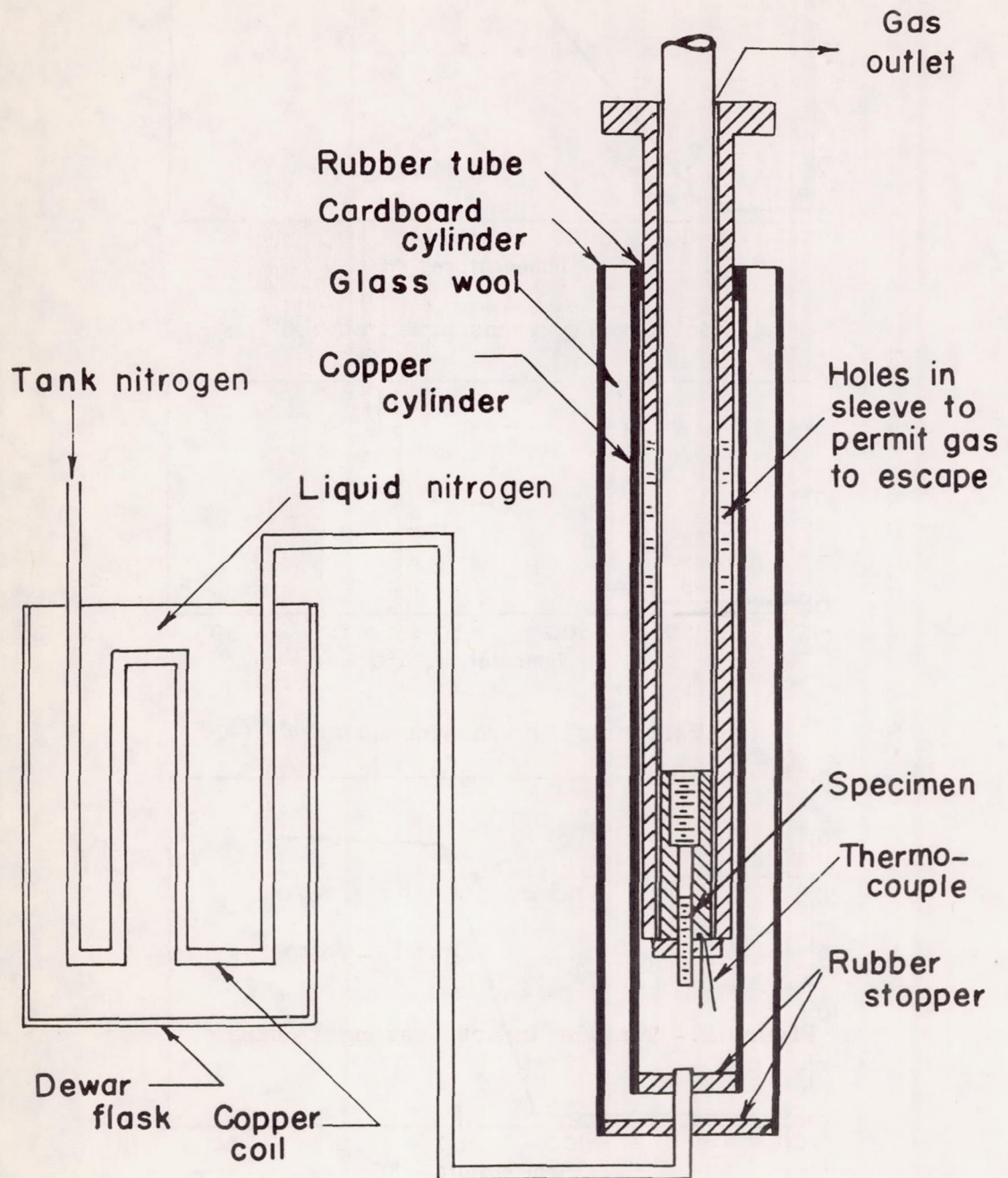
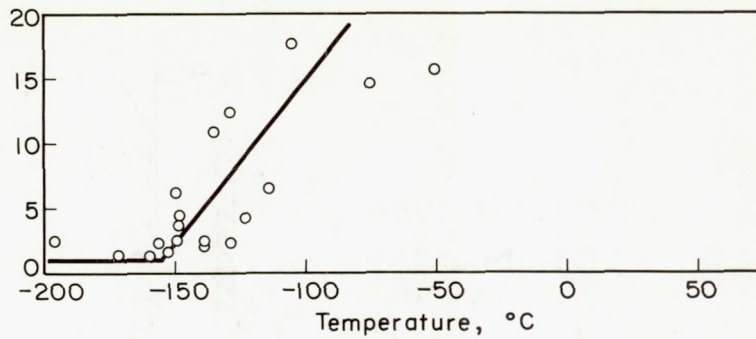
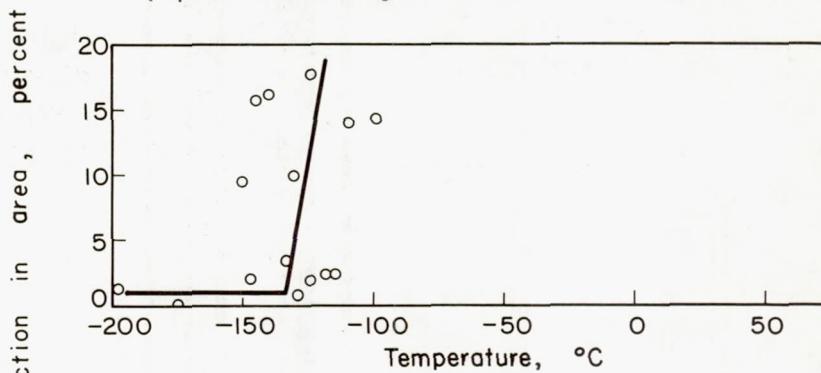


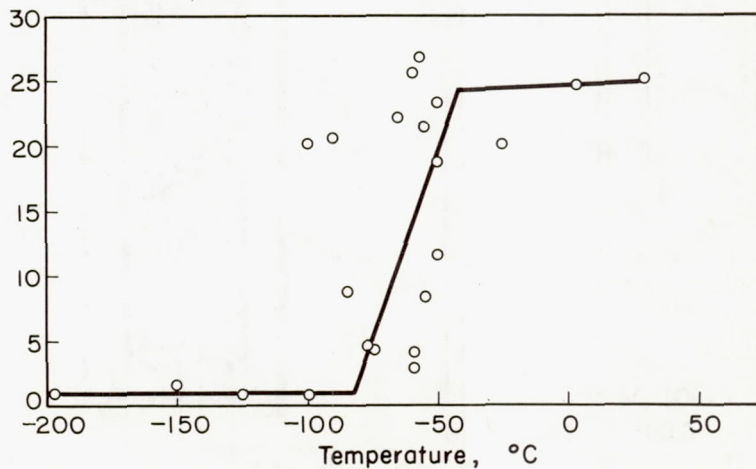
Figure 2.- Low-temperature-testing apparatus.



(a) Isothermally transformed at 490° C.

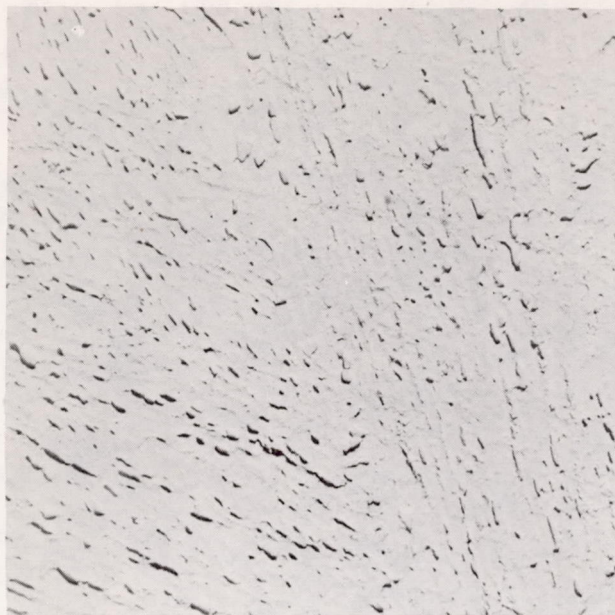


(b) Isothermally transformed at 445° C.

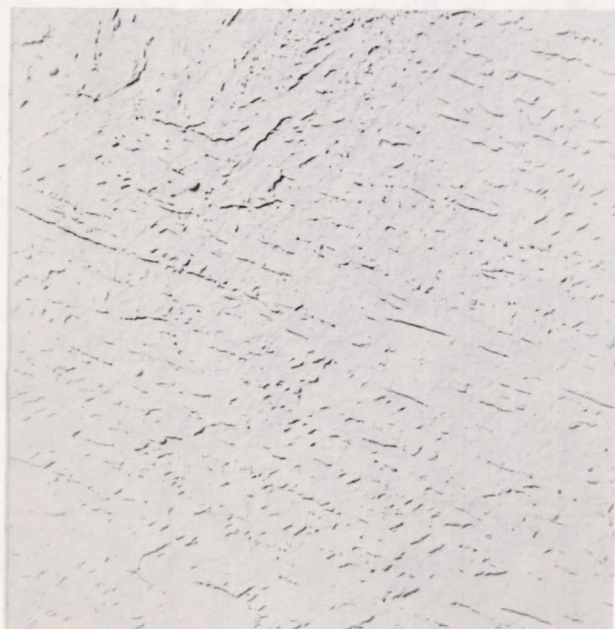


(c) Isothermally transformed at 405° C.

Figure 3.- Reduction in area in tensile impact against test temperature for steel 15 (0.21 percent carbon, 0.24 percent molybdenum) isothermally transformed at three temperatures.



(a) Steel 16 transformed at 405° C. Magnification, 10,000X.



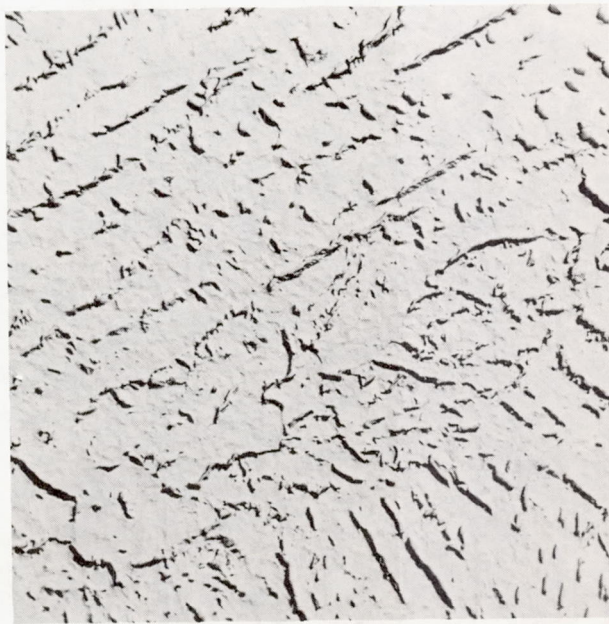
(b) Steel 16 transformed at 445° C. Magnification, 7,000X.

L-57-3039

Figure 4.- Electron micrographs.



(c) Steel 22 transformed at 350° C. Magnification, 9,000X.



(d) Steel 22 transformed at 480° C. Magnification, 7,000X.

L-57-3040

Figure 4.- Continued.



(e) Steel A transformed at 350° C. Magnification, 22,000X.



(f) Steel A transformed at 500° C. Magnification, 15,000X.

L-57-3041

Figure 4.- Concluded.

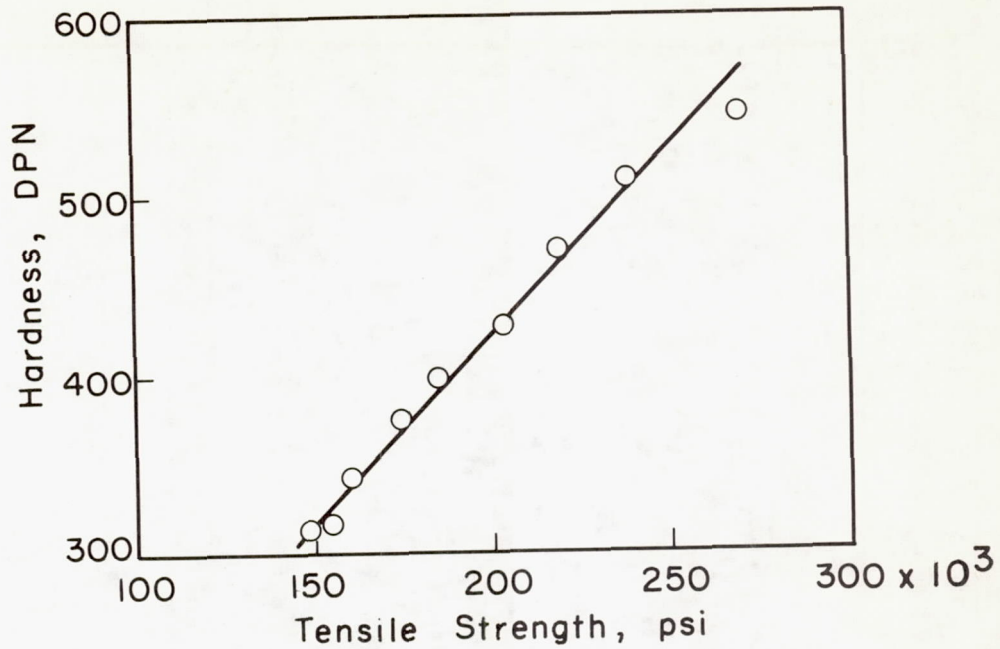


Figure 5.- Diamond pyramid hardness against tensile strength of bainite. Steel A.

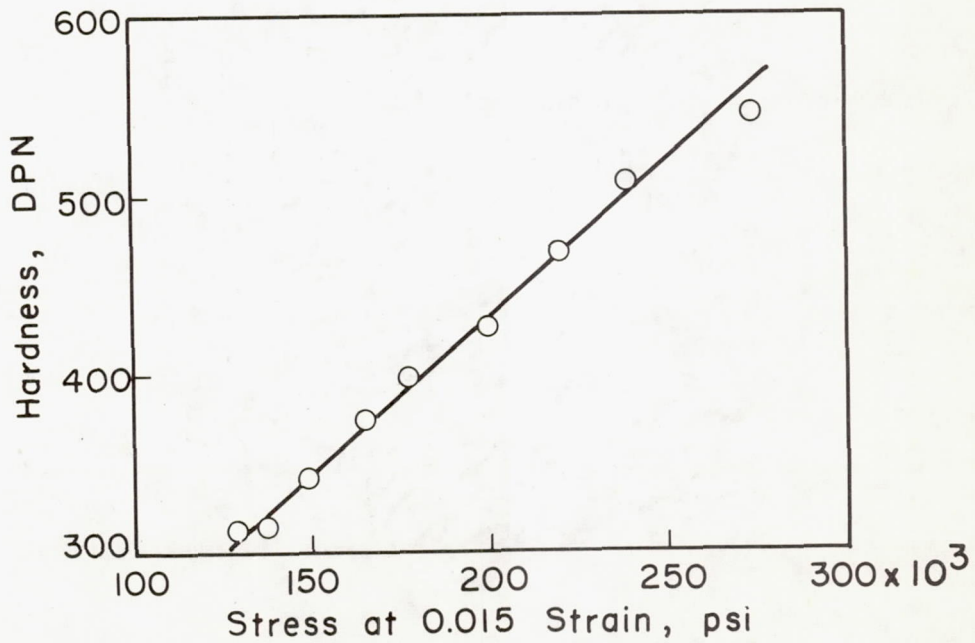


Figure 6.- Diamond pyramid hardness against stress at 0.015 strain in bainite. Steel A.

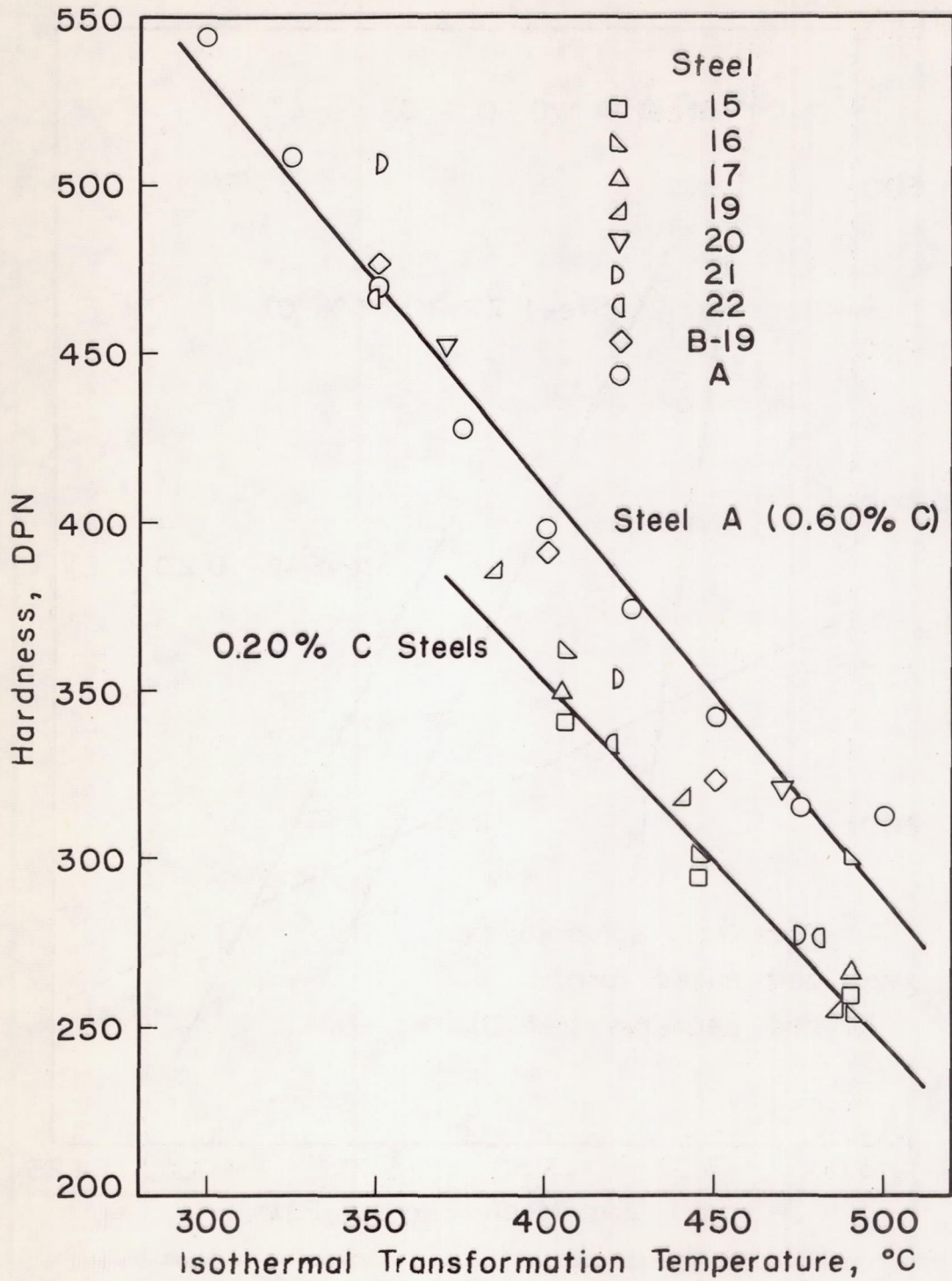


Figure 7.- Diamond pyramid hardness against isothermal transformation temperature for nine bainitic steels.

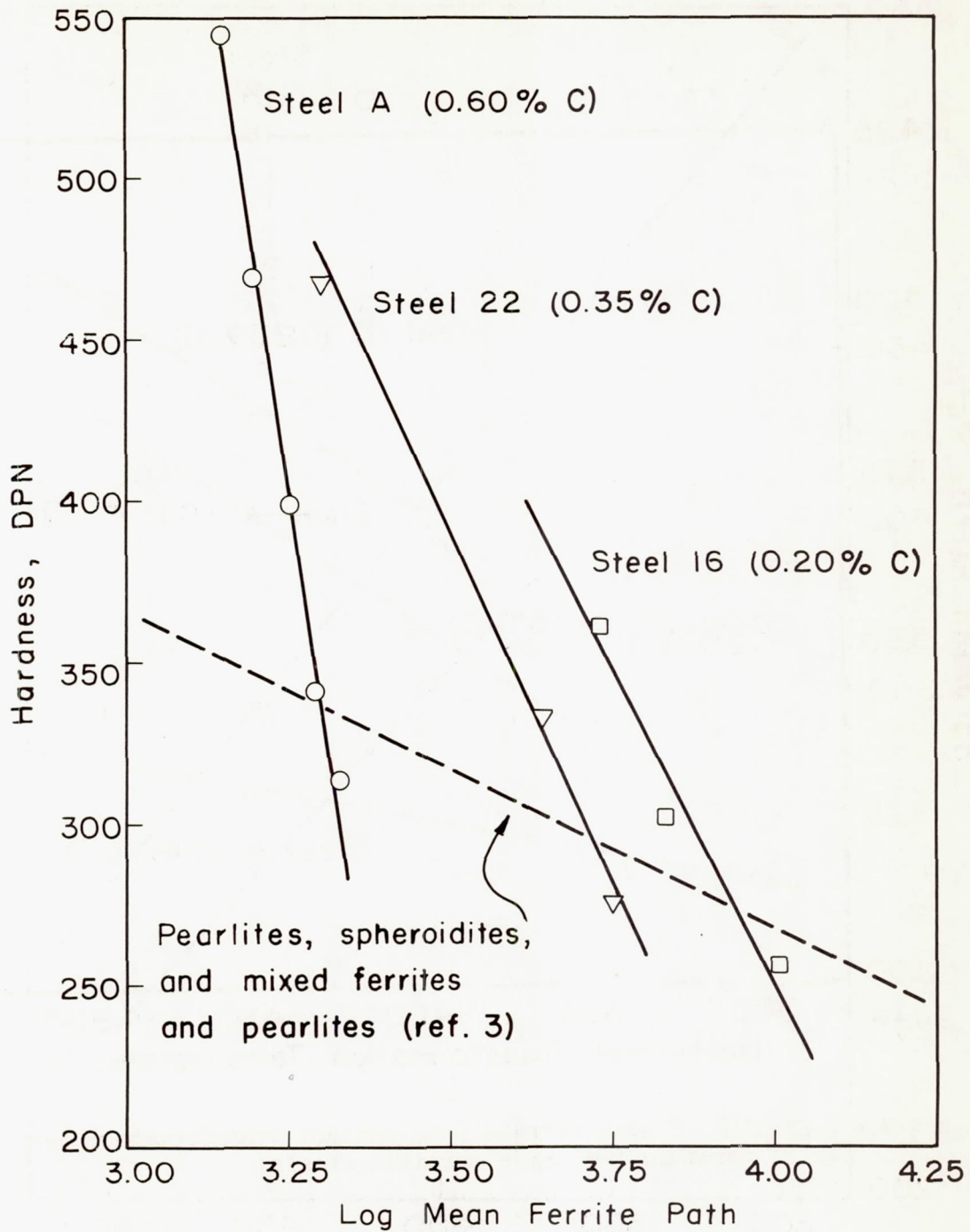


Figure 8.- Diamond pyramid hardness against logarithm of mean ferrite path for three bainites with curve for one pearlite given for comparison.

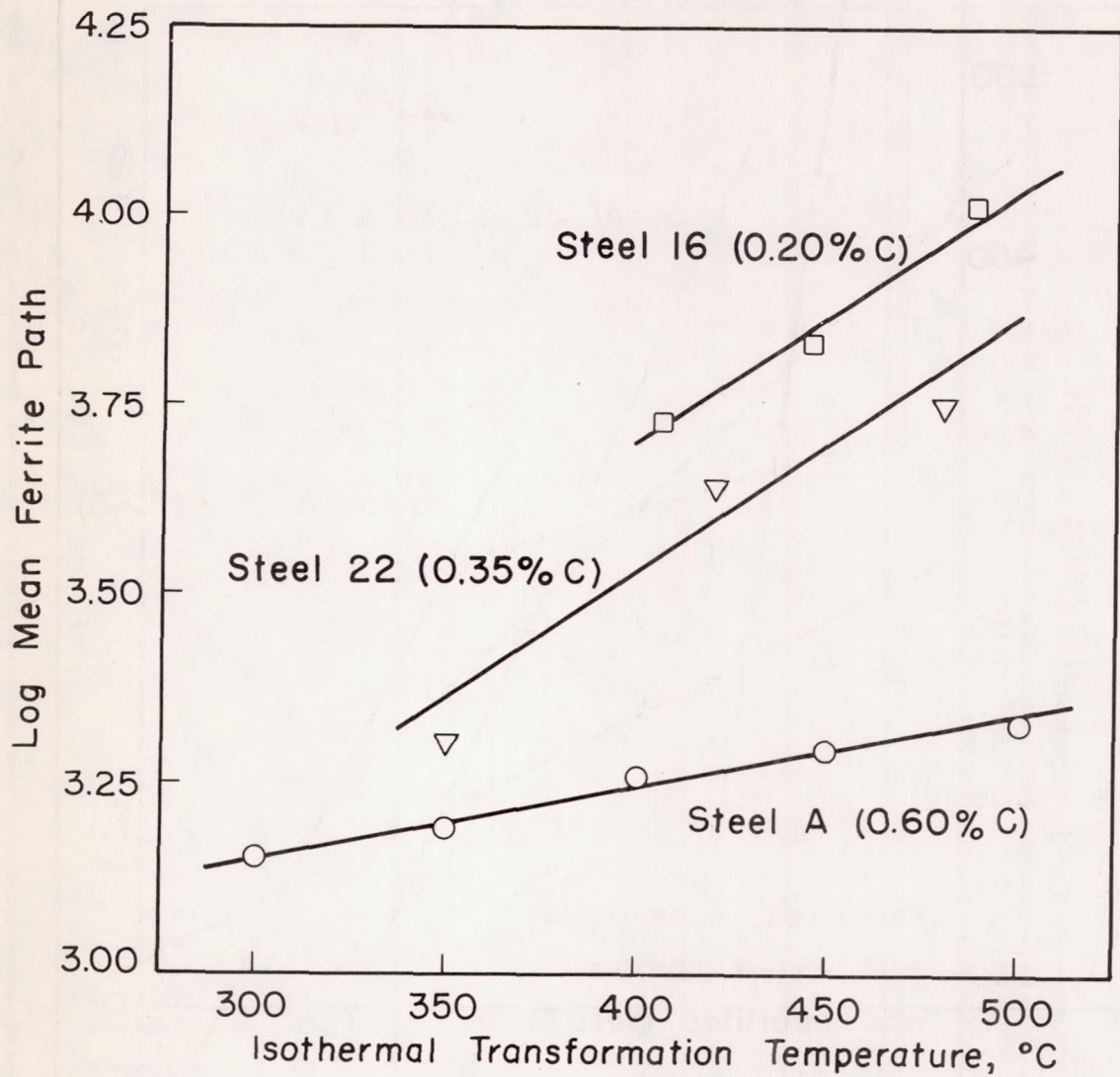


Figure 9.- Logarithm of mean ferrite path against transformation temperature for three bainitic steels.

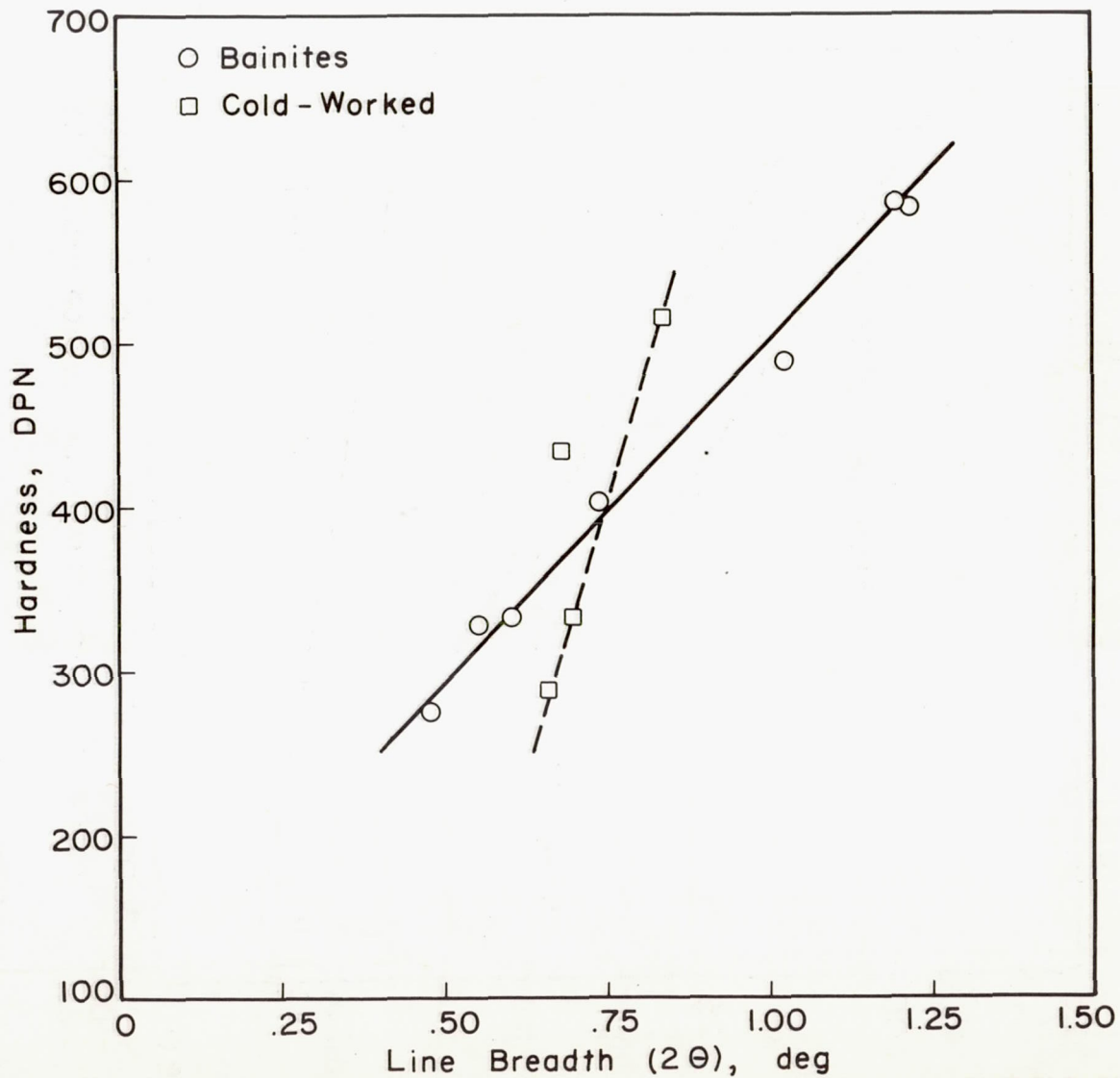
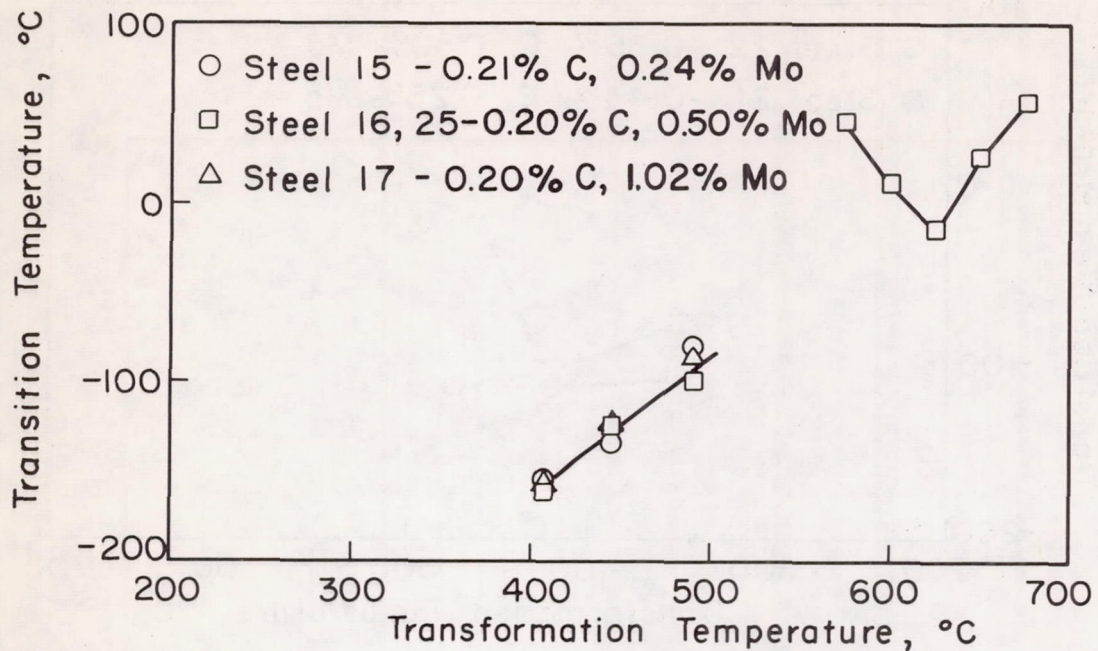
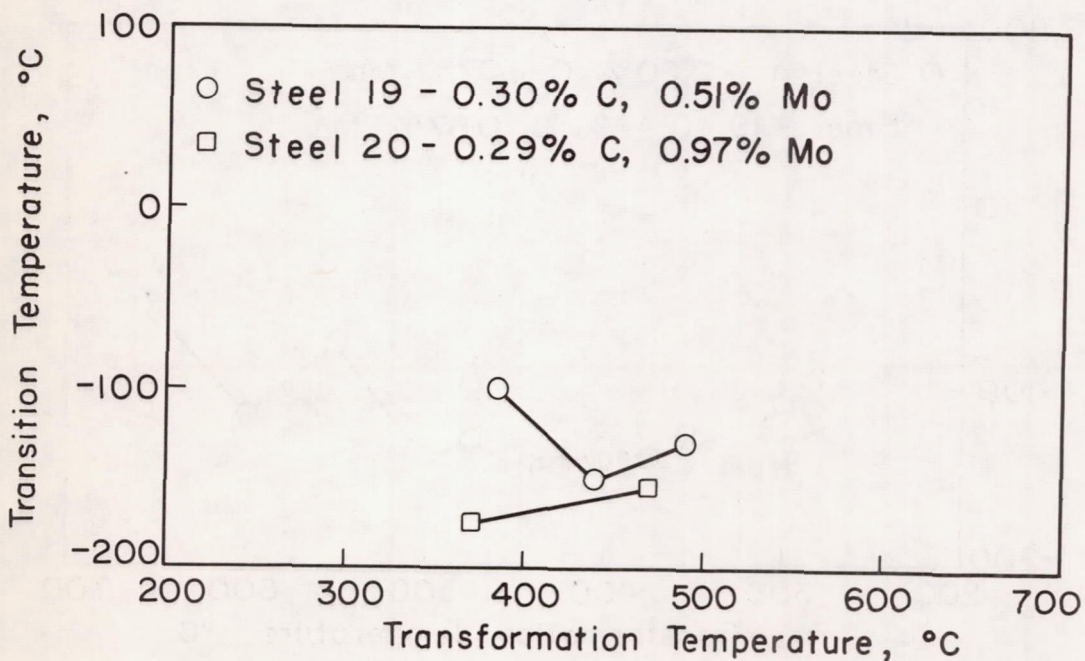


Figure 10.- Diamond pyramid hardness against X-ray line breadth of the (211) line for steel A hardened either by transforming to bainite or by cold-work.  $\theta$  is the Bragg angle.

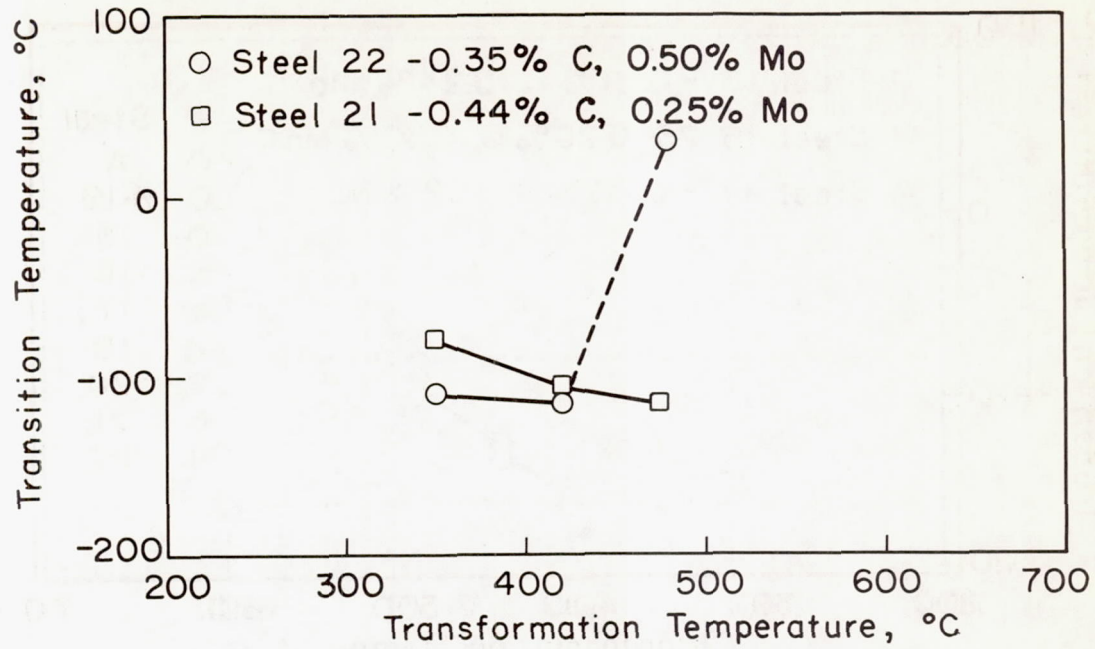


(a) 0.20-percent-carbon steels.

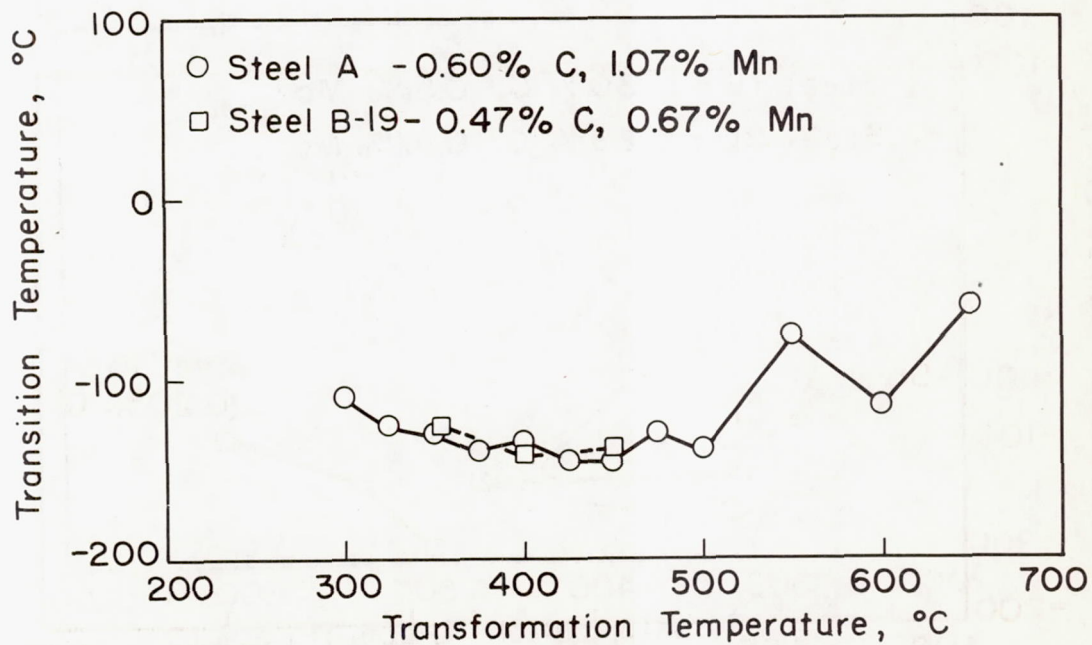


(b) 0.30-percent-carbon steels.

Figure 11.- Transition temperature against transformation temperature.



(c) 0.35- and 0.44-percent-carbon steels.



(d) 0.47- and 0.60-percent-carbon steels.

Figure 11.- Concluded.

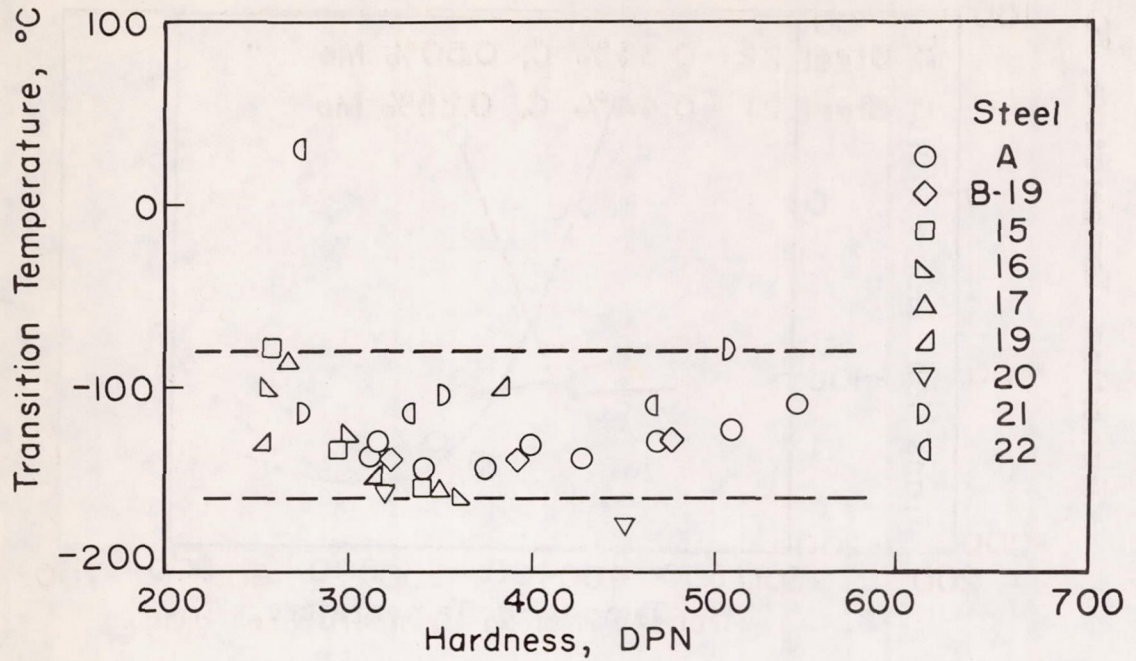


Figure 12.- Transition temperature against diamond pyramid hardness for bainitic steels.

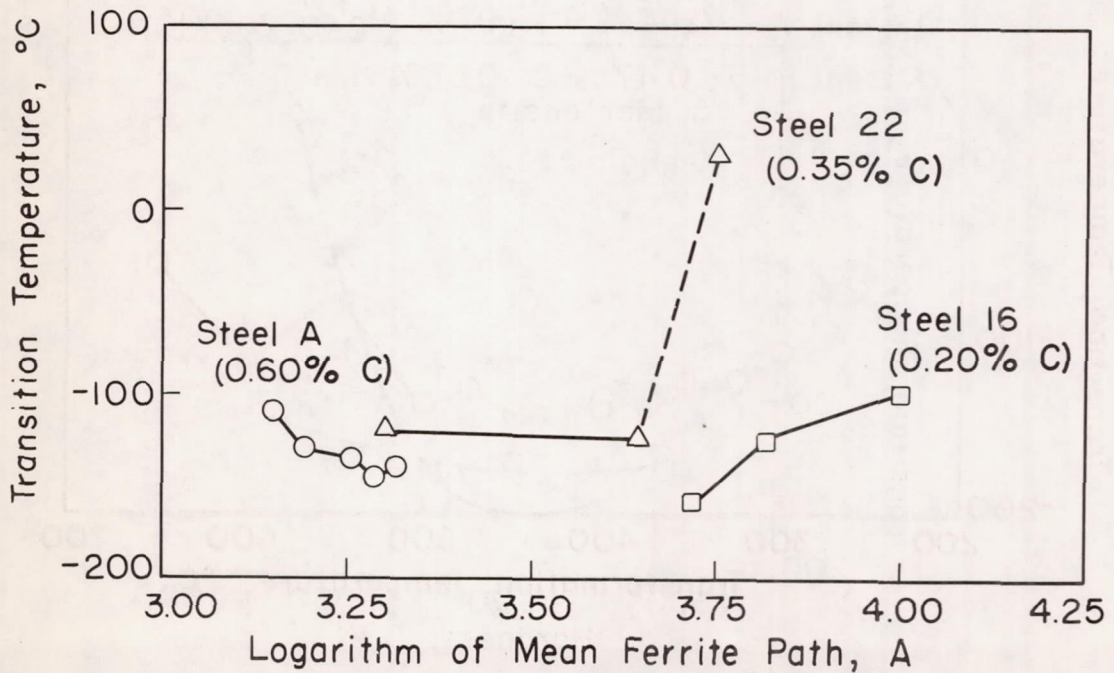


Figure 13.- Transition temperature against logarithm of mean ferrite path for three steels.

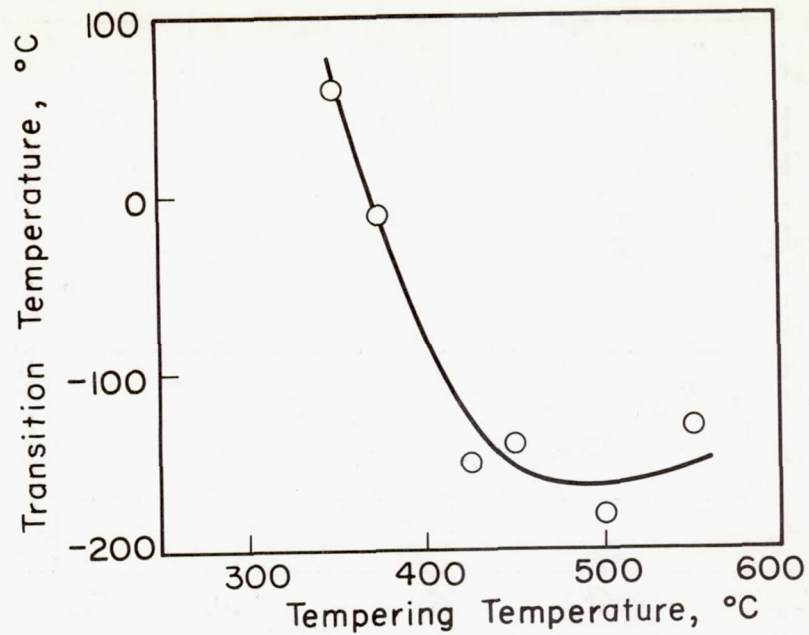


Figure 14.- Transition temperature against tempering temperature for tempered martensite. Steel A.

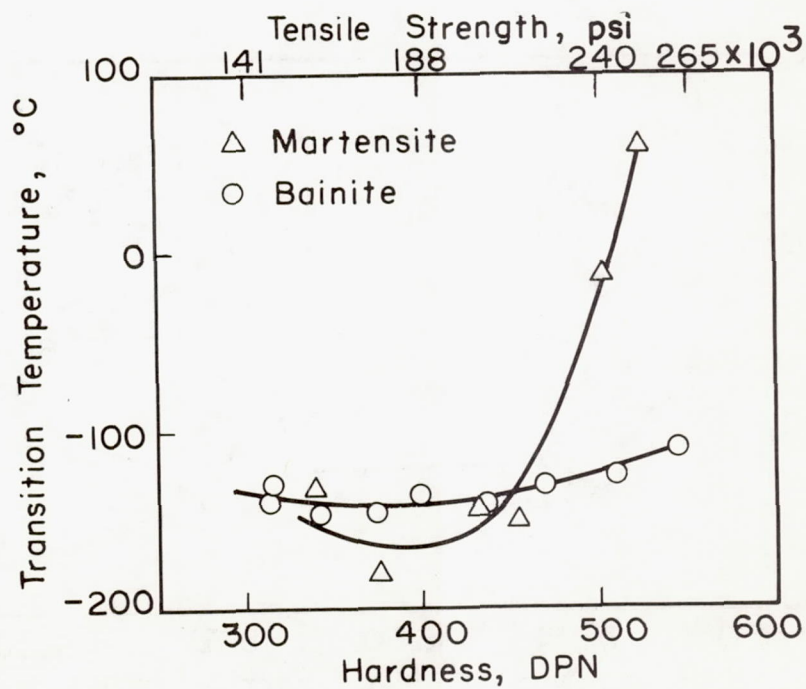


Figure 15.- Transition temperature against diamond pyramid hardness and tensile strength for bainite and tempered martensite. Steel A.